Contents lists available at ScienceDirect

Environmental Research

journal homepage: www.elsevier.com

Optimization and comparison of three spatial interpolation methods for electromagnetic levels in the AM band within an urban area

Montaña Rufo*, Alicia Antolín, Jesús M. Paniagua, Antonio Jiménez

Department of Applied Physics, School of Technology, University of Extremadura, Avda. de la Universidad s/n, 10003 Caceres, Spain

ARTICLE INFO

Keywords:
Electromagnetic radiation
Exposure assessment
Interpolation methods
Exposure quotient
Spectral analysis
GIS

ABSTRACT

A comparative study was made of three methods of interpolation – inverse distance weighting (IDW), spline and ordinary kriging – after optimization of their characteristic parameters. These interpolation methods were used to represent the electric field levels for three emission frequencies (774 kHz, 900 kHz, and 1107 kHz) and for the electrical stimulation quotient, Q_E, characteristic of complex electromagnetic environments. Measurements were made with a spectrum analyser in a village in the vicinity of medium-wave radio broadcasting antennas. The accuracy of the models was quantified by comparing their predictions with levels measured at the control points not used to generate the models. The results showed that optimizing the characteristic parameters of each interpolation method allows any of them to be used. However, the best results in terms of the regression coefficient between each model's predictions and the actual control point field measurements were for the IDW method.

1. Introduction

With the current growth of the world of communications, human exposure to electromagnetic radiation is increasing rapidly. This is raising public concern about the possible harmful effects of such radiation on health. Faced with this concern, the scientific community has responded by carrying out research determining the levels to which the general public is exposed in their daily life, and comparing these levels with the exposure limits published by the International Commission on Non-Ionizing Radiation Protection (ICNIRP, 2010, 1998), the Federal Communications Commission (FFC) (Cleveland and Ulcek, 1999), the Institute of Electrical and Electronics Engineers (IEEE Standard, 2005) the European Union (Recommendation, 1999) and the regulations adopted by some individual countries.

Some recent studies have considered the total electric field levels in different towns (Calvente et al., 2015; Paniagua et al., 2013), and others the electromagnetic radiation to which the population is exposed depending on the frequency of that radiation (Rufo et al., 2011). There have been dosimetric studies of the electric field levels to which an inhabitant is exposed in their daily life, using personal exposimeters (Bhatt et al., 2016a, 2016b; Gajšek et al., 2013; Joseph et al., 2010).

However, the results of these investigations are not available to the general public. Instead, the recipients of this information are themselves scientists, so that the fears of the population remain unresolved. Not only is the information not readily accessible, but the results of these many research papers are difficult to extrapolate from one scenario to another. One way of overcoming these problems is to represent the electric field levels in a geographic information system (GIS) (Aerts et al., 2013). GIS's have been used for the representation of a variety of parameters, such as continuous wind speed surfaces (Luo et al., 2008), surface temperature (Tiengrod et al., 2013), water quality (Aminu et al., 2015), and electromagnetic field levels in different towns (Azpurua and dos Ramos, 2010; De Doncker et al., 2006; Paniagua et al., 2013). Some studies have compared different interpolation methods for such different variables as daily global solar radiation (Jeong et al., 2017), surface temperature (Tiengrod et al., 2013), and average electromagnetic field magnitude (Azpurua and dos Ramos, 2010). However, which method best reproduces the measured values can depend on such aspects as data density, spatial distribution of samples, and temporal variation, inter alia (Bennett et al., 2013; Li and Heap, 2014).

One of the most important factors in generating a spatial model is to be able to indicate its associated accuracy (Kirchner et al., 1996). For this, the results of the model need to be compared with a source of

* Corresponding author.
Email address: mmrufo@unex.es (M. Rufo)

https://doi.org/10.1016/j.envres.2018.01.014
Received 27 November 2017; Received in revised form 12 January 2018; Accepted 15 January 2018
Available online xxx
0013-9351/

greater accuracy. In the present case, this source was quantification at control points, i.e., points at which field measurements were made but not used in the generation of the different models.

The main objective of this work was to optimize and compare three different models of the electric field levels in a given study area. The models were generated using the ArcGIS 9.2 program, considering three interpolation methods for study: inverse distance weighting (IDW), ordinary kriging and spline. The parameters defining these interpolation methods were analysed to maximize the accuracy of the corresponding models. We then used ArcGIS to compare the values measured in the field at a set of control points with the predictions of the different models at those points. (As noted above, the control point data were not used at any time for the computation of the various maps or models).

The analysis of the results was centred on calculating the mean absolute error (MAE), mean square error (MSE), and root-mean-square error (RMSE). In addition, linear fits were made of the values predicted by the different models to the measured values, quantifying the value of the regression coefficient, *r*. Finally, we studied the percentage error obtained with the three models for each of the emissions and the electrical stimulation quotient, Q_E.

2. Material and methods

2.1. Sampling procedure

The study was conducted in a village, Valdesalor, situated near the city of Cáceres, at 39.377938°N, 6.347946°W (Fig. 1). Its area is 0.16 km^2. The fundamental characteristic of this village is that, although it has only 600 inhabitants, it is just 3 km from a site of MW antennas. The site has two medium-wave radio broadcasting transmitters with effective radiated powers (ERP) of 60 and 25 kW, and frequencies of 774 and 1107 kHz, respectively. Farther away, at about 8.5 km from the village, there is another site with an antenna of 10 kW ERP and 900 kHz frequency (Royal Decree, 1993).

We selected 52 measurement points in the village, distributed in accordance with the communication routes (Maling, 1989) throughout the village. The electric field associated with each of the aforementioned three antennas (774 kHz, 900 kHz, and 1107 kHz) was determined at each of these points. In addition to the measurement points, 18 control points were chosen at which field measurements were made, but not used in generating the different models. These points served to obtain the deviation of the predicted values given by the model from those actually measured in the field. The measurement and control points were included, together with a digital map, in a GIS. Fig. 2 shows the digital map with the measurement points.

In order to get a measure of the temporal stability of the data, 12 systematic measurements were made at one of the measurement points on different days covering the duration of the study. In this way, we could get an estimate of the error associated with the source's emission stability as well as the influence of the presence of vehicles or people in the measurement environment.

A spectrometric analysis was performed at all points using an R&S FSH3 spectrum analyser. This is sensitive in the frequency range 100 kHz–3 GHz, and it has a dynamic range from −114 dBm to + 30 dBm, a resolution bandwidth from 1 kHz to 1 MHz, and an overall amplitude accuracy of 0.5 dB. The antenna used with this analyser was a passive monopole [ETS-LINDGREN (EMCO) model 3303] with a frequency range 0.001–30 MHz and standard uncertainty 0.05 dB. The antenna was situated on a dielectric tripod at 1.5 m above ground level with vertical polarization. Spectra were acquired in the frequency range 0.5–3.5 MHz with bandwidth resolution (RBW) of 10 kHz and sweep time 100 ms (ECC, 2006). The measurements were made in max-hold and peak mode, recording the peak trace over a 6-min period at each point, according to the recommendation of Electronic Communication Committee (ECC, 2006).

Fig. 1. The village of Valdesalor, with the locations of the medium-wave radio broadcasting antennas (774 kHz, 900 kHz, and 1107 kHz).

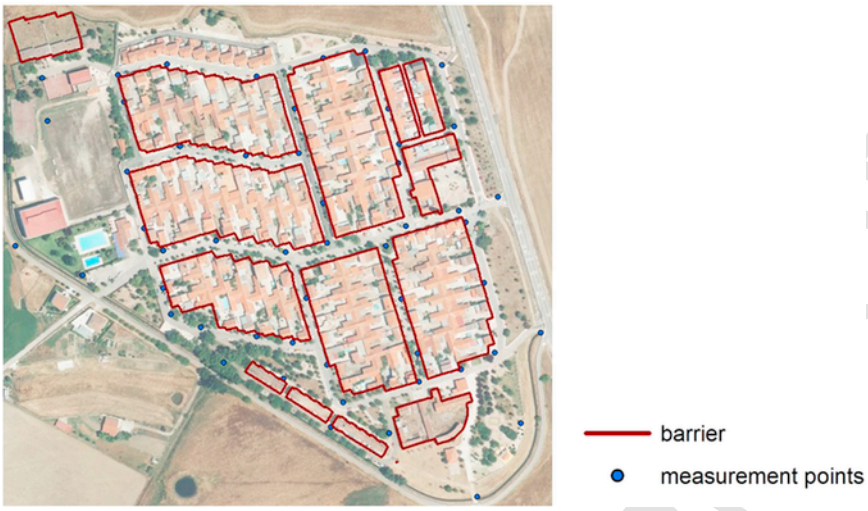

Fig. 2. Digital map of the village of Valdesalor with the measurement points distributed throughout the locality.

2.2. Data processing

The voltage signals V [dB(μV)] detected by the spectrum analyser were converted to electric fields E using Eq. (1):

$$E\left[dB\left(\mu V/m\right)\right] = K\left[dB\left(1/m\right)\right] + V\left[dB\left(\mu V\right)\right] + L_r\left[dB\right] \quad (1)$$

where K is the antenna factor included in the calibration certificate provided by the manufacturer and L_r represents the cable losses that is negligible at these frequencies. The power density S was calculated using Eq. (2):

$$S = E^2/Z_0 \quad (2)$$

where Z_0 is the impedance of the free space, $Z_0 = 120{\cdot}\pi\ \Omega$, and all the measurements are considered to correspond to the far field regime.

The measurement uncertainty $u_c(E)$ was evaluated as the square root of the weighted sum squares (Eq. (3)):

$$u_c\left(E\right) = \sqrt{\sum_{i=1}^{n}\left(c_i \cdot u_{xi}\right)^2} \quad (3)$$

where u_{xi} is the standard uncertainty and c_i are the sensitivity coefficients for the estimates x_i of each quantity, used to multiply the input quantities so as to express them in term of the output quantity (ECC, 2006).

The expanded measurement uncertainty u_e is calculated from the combined standard uncertainty as:

$$u_e\left(E\right) = 1.96 \cdot u_c \quad (4)$$

The combined standard uncertainty, calculated taking into account the calibration of the spectrum analyser (0.5 dB) and the monopole antenna (0.05 dB), was found to be 0.5 dB, and the expanded uncertainty 0.8 dB. In SI units, this expanded uncertainty implies a relative error of 12% for the electric field and 24% for the power density.

To calculate the levels of electromagnetic field exposure to which people are subject, it is necessary to compare the measured fields with reference levels. To this end, we used the ICNIRP power-density reference levels for the general public. Their mathematical expressions are given in Table 1 for the frequency ranges used in the present work (ICNIRP, 1998, 2010).

Table 1
Reference levels for the general public exposure to time-varying E-field strength in the frequency range 0.15 MHz – 300 GHz, with f as indicated in the frequency range column (ICNIRP, 2010, 1998).

Frequency range	E-field strength (V/m) ICNIRP (1998)	E-field strength (V/m) ICNIRP (2010)
3 kHz to 1 MHz	87	83
1–10 MHz	$87/f^{1/2}$	83

According to the ICNIRP (ICNIRP, 2010), the criterion for exposure to multiple-frequency sources to prevent electrical stimulation and thermal effects should take into account the electric and the magnetic fields. But, as we have concluded in previous work, the limiting criterion for preventing electrical stimulation is stricter than the thermal criterion, and the exposure quotients are closer to unity for the electric field than for the magnetic field at environmental levels (Paniagua et al., 2009). For this reason, in the present work we shall focus on the study of the electric field exposure coefficients. These coefficients are calculated either according to Eq. (5),

$$Q_E = \sum_{i=1}^{1}{}^{MHz}_{Hz}\frac{E_i}{E_{L,i}} + \sum_{i>1}^{10}{}^{MHz}_{MHz}\frac{E_i}{a} \le 1 \quad (5)$$

Where E_i is the electric field strength at frequency i, and $E_{L,i}$ is the electric field reference from Table 1 and a is 87 V/m for general public exposure (ICNIRP, 1998).

Or according to Eq. (6),

$$Q_E = \sum_{i=1}^{1}{}^{MHz}_{Hz}\frac{E_j}{E_{R,j}} \le 1 \quad (6)$$

Where E_j is the electric field strength induced at frequency j, and $E_{R,j}$ is the electric field strength reference level at frequency j as given in Table 1 (ICNIRP, 2010).

2.3. Spatial analysis

An interpolation method estimates the values of a given magnitude at points where it has not been measured, using data of that magnitude at other relatively close points. Spatial interpolation assumes that the variation in magnitude is continuous in space. This section introduces

the different interpolation methods used in this study. These were: inverse distance weighting (IDW), spline and ordinary kriging.

2.3.1. Inverse distance weighting (IDW)

This method of interpolation considers the positive influence of the nearest points. Those measured values closest to the prediction location will have more influence on the predicted value than those farther away (Luo et al., 2008). Given that IDW uses average values, the resulting values for the interpolated cells will never exceed the maximum and minimum limits of the input interpolating data. IDW estimates the values of the pixels by averaging the known interpolating data. The number of points to take into account and their positions will be defined on the basis of a geostatistical analysis of the data. To estimate the interpolated cells in ArcGIS, one has to define the following parameters: power, search radius (fixed or variable), number of points, and barriers.

2.3.2. Spline interpolation

This generic interpolation method fits a minimum curvature surface through the known interpolating points (Egerstedt and Martin, 2010). It is usually applied to define gradual variations of surfaces. It may not, however, be the best method of interpolation when there are large variations over relatively short horizontal distances. There are two options in spline interpolation: regularized or tension. On the one hand, the regularized method allows the smoothness of the surface to be controlled. The parameters on which one can act are weight and number of points. Weight allows the smoothness of the surface to be adjusted, and is used to minimize surface curvature, with greater values resulting in smoother surfaces. The number of points controls the average number of points contained in each region used in the calculation of the surface. On the other hand, the tension method fits a surface to a set of points. The surface is taken to be a thin sheet of slightly elastic material deformed to fit the points. In a tension spline, the elasticity of the surface can be controlled. The parameters on which one can act are the same as in the regularized option – weight and number of points.

2.3.3. Ordinary kriging

Kriging is a stochastic technique in that it uses a linear combination of weights at known points to estimate the value at an unknown point. In contrast with the other two methods which are deterministic, kriging is a geostatistical method (Luo et al., 2008). Kriging provides a solution to the problem of estimating the surface by taking spatial correlation into account. To this end, it uses a semivariogram, a measure of spatial correlation between two points in which the weights vary according to the spatial arrangement of the samples. The semivariogram can be a function of both distance and direction, and can thus account for direction-dependent variability. Before computing the models, we performed a study of the normality, the anisotropy, and the variogram of the experimental data. The software takes this prior analysis into account in generating the models, as well as whether or not it is necessary to apply a logarithmic transformation to the samples. To determine the weights of nearby data in computing the interpolated values, we applied the spherical variogram model since this is the most extensively used variogram option (Cressie, 1993), getting spatial continuity in the N-S direction and an anisotropic spatial pattern.

For the accuracy analysis of the spatial extrapolation methods, we calculated the MAE, MSE, and RMSE in accordance with Eqs. (7)–(9), as well as the regression coefficient r between each model's predictions and the actual control point field measurements.

$$MAE = \frac{1}{N}\sum_{i=1}^{N}\left|E(x,y) - E_i\right| \tag{7}$$

$$MSE = \frac{1}{N}\sum_{i=1}^{N}(E(x,y) - E_i)^2 \tag{8}$$

$$RMSE = \sqrt{\frac{1}{N}\sum_{i=1}^{N}(E(x,y) - E_i)^2} \tag{9}$$

where $E(x,y)$ is the predicted value and E_i is the observed value at the control point.

The *MAE* was used to detect bias. It should ideally be zero if the predictions are unbiased, i.e. centred on the measurement values. The *RMSE* was used to compare different methods by seeing how closely predicted values match the measured values. The smaller the *RMSE* the better.

3. Results and discussion

The village studied has, as mentioned above, a site of AM antennas at close range. This means that the distribution of electromagnetic field exposure is largely due to AM frequency emissions ([0.001–30] MHz).

Fig. 3 shows by way of example the spectrum for the medium wave band of the electric field measured at a point in the centre of the village. This spectrum is representative of the general trend of the spectra collected in the village for the frequency band studied. One clearly observes the 774 kHz, 900 kHz, and 1107 kHz signals, and one can appreciate that the electric field is greater for the 774 kHz and 1107 kHz signals due to the proximity of the emitting sources and their ERPs of 60 kW and 25 kW, respectively.

Twelve measurements were made at one of the points in the village on different days covering the duration of the study. The aim was to check whether the electric field levels remained stable or presented some temporal trend. Table 2 gives the descriptive statistics of this temporal variation study. The measured fields fluctuated randomly during the sampling period, and no temporal trend was detected. As can be seen in the table, the coefficient of variation is between 23% for the 774 kHz emission and 37% for the 1107 kHz emission. These values are greater than the expanded uncertainty calculated taking into account the calibration of the spectrum analyser and the monopole antenna, which was between −11% and +12% for the electric field.

As described in "Materials and Methods", electric field measurements were made for the three emissions (774 kHz, 900 kHz, and 1107 kHz) at 52 points distributed throughout the village. The maximum values detected were 4.57 V/m, 0.13 V/m, and 2.19 V/m for

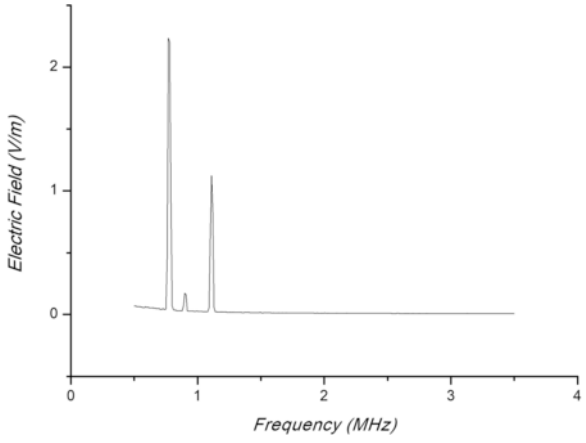

Fig. 3. Spectrum measured at a point of the urban centre of Valdesalor where in which one observes the 774, 900 and 1107 kHz signals.

Table 2
Statistical summaries of the electric fields measured at a point of the town in the temporal study. Sample size: 12.

	$E_{774\ kHz}$	$E_{900\ kHz}$	$E_{1107\ kHz}$	$Q_{E\ 1998}$	Q_{E2010}
Range (V/m)	0.50 – 0.68	$4.44\ 10^{-2}$–$8.67\ 10^{-2}$	0.16–0.28	$0.83\ 10^{-2}$–$1.14\ 10^{-2}$	$0.87\ 10^{-2}$–$1.20\ 10^{-2}$
Average (V/m)	0.59	$6.23\ 10^{-2}$	0.21	$9.71\ 10^{-3}$	$1.02\ 10^{-2}$
SD (V/m)	0.07	$1.03\ 10^{-2}$	0.04	$1.14\ 10^{-3}$	$1.19\ 10^{-3}$
Median (V/m)	0.56	$6.06\ 10^{-2}$	0.20	$9.36\ 10^{-3}$	$9.81\ 10^{-3}$
CV (%)	22.9	32.4	37.4	23.0	23.0

these frequencies, respectively. Fig. 4 is a box-and-whisker plot synthesis of the statistics (range, first and third quartiles, median, and mean) of the electric field for each frequency signal. One observes in the figure that the electric field values for the 774 kHz and 1107 kHz emissions are greater than those for the 900 kHz emission. This can simply be understood as a result of the antenna of this last emission both being further away than the others from the measurement points and having a lower ERP, 10 kW. Specifically, the values of the electric field for the 774 kHz emission are in the range 0.53–4.57 V/m with a median of 1.81 V/m. For the 900 kHz emission in the range 0.05–0.31 V/m with a median of 0.14 V/m, and for the 1107 kHz emission in the range 0.16–2.19 V/m with a median of 0.73 V/m. The coefficients of variation for these frequencies are 50%, 44%, and 52%, respectively, all greater than the respective values obtained in the temporal study. It is known that medium wave signals propagate primarily as ground waves, and are therefore less affected by attenuation inside the city than when propagation is by line of sight (Seybold, 2005). In the present study, however, there were no significant correlations between the measured electric field values and the distances to each of the emitting antennas because the differences in these distances to the antennas were relatively small. Given the linear correlation found between them ($m = 2.09 \pm 0.12$, $n = 0.21 \pm 0.11$, $r = 0.922$), the spatial variations in the 1107 kHz and 774 kHz emission electric field levels seem to be affected by the same parameters. For this reason, we consider that the spatial variations that we observed are mainly due to the shielding effect of the buildings in the village, and to a much smaller extent to the variation in the distance to the antennas.

All the electric field values measured in the study are below the limits established by the ICNIRP. These are 87 V/m for the 774 and 900 kHz emissions and 82.7 V/m for the 1107 kHz emission (ICNIRP, 1998), and generally slightly lower, 83 V/m, for the three emissions in the ICNIRP, 2010 update (ICNIRP, 2010). However, an appropriate dosimetric evaluation would require applying the criteria given in Eqs. (5) or (6) to limit exposure taking into account the effects of electrical

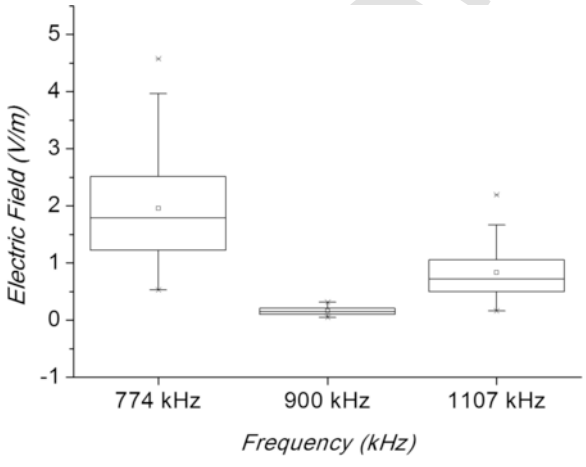

Fig. 4. Box and whiskers plot of the electric fields (V/m) for each frequency (774, 900 and 1107 kHz).

Table 3
Statistical summaries of the electrical stimulation quotients, Q_E, and power densities, $S(\mu W/cm^2)$, in the spatial study.

	Electrical Stimulation Q_E		$S(\mu W/cm^2)$
	Exposure quotient $(x10^{-3})$	*Times below*	
Mean	33.9	30	1.50
Median	31.4	30	1.04
Minimum	8.8	100	0.08
Maximum	80.9	10	6.84
SD	16.6	–	1.48
Size	52		52

stimulation. Table 3 presents a summary of the statistics (mean, median, minimum, maximum, and standard deviation) of Q_E and S, Eqs. (5) and (2) respectively, obtained from the spatial study data. One observes that the established limiting criteria are complied with. Indeed, even in the worst case, the Q_E quotient is more than 10-fold lower than the limit.

The values of mean and median in our study are $33.9\ 10^{-3}$ and $31.4\ 10^{-3}$. These lie within the range we found in studies conducted over a larger area centred on the same antenna site (Paniagua et al., 2012, 2010). The present results are also coherent with our previous observation of no dependence of the electric field intensity on distances when these were less than 10 km (Paniagua et al., 2012).

3.1. Spatial analysis

The interpolation methods used in our study were: IDW, spline, and ordinary kriging. Fig. 5 shows, by way of example, the model obtained for the 774 kHz electric field using the IDW method, optimizing the different parameters so as to obtain the most favourable case. In this model, the ArcGIS software applied a prior logarithmic transformation to the data. The fixed radius value of 75 m was selected in accordance with the variogram obtained, as also was the separation between the interpolated points. In addition, barriers were used to limit interpolation between points separated by buildings.

As can be seen in the figure, the highest values detected are distributed in the outermost parts of the village, a fact that seems to indicate that the buildings shield the electric field. This result was obtained for all three methods and all three frequencies analysed. Indeed, the lowest values are in the central part of the village for all of the emissions. Table 4 presents a statistical summary of the results, with the values of MAE, MSE, RMSE, and m (slope), n (intercept), and r (correlation coefficient) for the straight line fit of the predicted values to those actually measured at the control points.

The values in Table 4 show that, for all the cases studied, the best methods seem to be ordinary kriging and IDW. These two methods give smaller RMSE and Q_E values for the different emission frequencies. The MAE values were of the same order of magnitude for all three methods. By emission frequency, the MAE's obtained for the 900 kHz emission are the smallest. This is because the range of values obtained for this frequency is smaller than for the other two emissions, 774 kHz and 1107 kHz, and this narrower range goes together with lower values of

Fig. 5. The IDW interpolated map of the E-field intensity for 774 kHz signal.

Table 4
Statistical summary of the three interpolation methods for each frequency (774, 900 and 1107 kHz) and the electrical stimulation quotients, Q_E.

Frequency	Method	MAE (V/m)	MSE $(V/m)^2$	RMSE (V/m)	m n	r
774 kHz	IDW	0.46	0.30	0.55	0.87 ± 0.32 0.42 ± 0.32	0.79
	Kriging	0.44	0.28	0.53	0.77 ± 0.14 0.61 ± 0.29	0.79
	Spline	0.47	0.41	0.64	0.83 ± 0.18 0.55 ± 0.36	0.73
900 kHz	IDW	$4.3\ 10^{-3}$	$3.1\ 10^{-3}$	$5.6\ 10^{-3}$	1.26 ± 0.28 −0.003 ± 0.04	0.73
	Kriging	$3.0\ 10^{-3}$	$1.5\ 10^{-3}$	$3.9\ 10^{-3}$	0.89 ± 0.20 0.03 ± 0.03	0.73
	Spline	$4.4\ 10^{-3}$	$3.9\ 10^{-3}$	$6.2\ 10^{-3}$	1.31 ± 0.31 0.09 ± 0.04	0.70
1107 kHz	IDW	0.20	0.06	0.23	0.79 ± 0.14 0.17 ± 0.13	0.81
	Kriging	0.21	0.06	0.24	0.67 ± 0.13 0.26 ± 0.12	0.79
	Spline	0.22	0.07	0.26	0.75 ± 0.14 0.22 ± 0.14	0.77
Q_E	IDW	$7.6\ 10^{-3}$	$8.2\ 10^{-5}$	$9.1\ 10^{-3}$	0.86 ± 0.15 0.007 ± 0.005	0.81
	Kriging	$6.7\ 10^{-3}$	$6.9\ 10^{-5}$	$8.2\ 10^{-3}$	0.61 ± 0.16 0.013 ± 0.005	0.70
	Spline	$7.4\ 10^{-3}$	$11.1\ 10^{-5}$	$10.5\ 10^{-3}$	0.82 ± 0.17 0.009 ± 0.006	0.74

MAE, MSE, and RMSE. With respect to the regression coefficient, the highest values in all cases are for the IDW method.

Fig. 6 is a plot of the IDW-predicted values of the electric field for the 1107 kHz emission versus the actual measurements at the control points. It also shows the best straight line fit, whose regression coefficients are given in Table 4.

Fig. 7 shows box-and-whisker plots of the percentage errors in the estimates, Eq. (10), made with the different optimized interpolation methods for the three emission frequencies and Q_E.

$$\left| \frac{E_{measured} - E_{interpolated}}{E_{measured}} \right| * 100 \tag{10}$$

For the 1107 kHz emission, the mean error for the most favourable case (IDW) is 26%, and the median is 24%. For the kriging and the spline models, the mean errors increase to 27% and 29%, respectively, and the medians are 23% and 24%, respectively. For the 774 kHz emission, there appears to be a smaller deviation of the data with the IDW model, whereas the spline seems clearly to give the poorest reproduction of the measured values. There appear to be greater differences in the 900 kHz emission case. The model that gives the best fit in this case is kriging with a mean error of 24%, while the IDW and spline models have mean errors of 33% and 35%, respectively. There appears to be less dispersion of the Q_E values with the kriging model, for which the mean error is 28%, while the spline model gives the greatest dispersion of these values.

In optimizing the modeling with the different methods, we obtained similar mean errors which in no case were greater than those corresponding to the temporal variation.

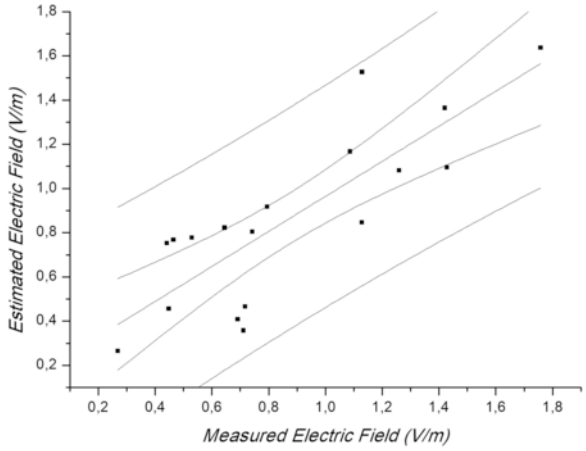

Fig. 6. Estimated Electric Field (V/m) versus measured Electric Field (V/m) for the 1107 kHz signal (solid discs) and straight line fit (solid line).

The values obtained for these variables are similar to those reported by (Azpurua and dos Ramos, 2010), although in their case the differences were greater for some of the models used, with the best method being the IDW. It should be noted that their study was of broadband levels, with no distinction by frequency.

4. Conclusions

In this study, we have characterized the levels of non-ionizing radiation in a village located 3 km from a site of two medium-wave radio broadcasting transmitters with a total effective radiated power of 85 kW. The electric field and the power density were quantified at 52 points in the village for three AM band emissions (774 kHz, 900 kHz, and 1107 kHz), obtaining maximum values of 4.57 V/m, 0.13 V/m, and 2.19 V/m, respectively. Simultaneously, a temporal study was carried out at one of the points of the village covering the duration of the spatial study. This gave temporal variations of 22.9%, 32.4%, and 37.4% for the above three emissions, respectively. These values are less than the corresponding spatial variations detected in the area, which were 50%, 44%, and 52% for the 774 kHz, 900 kHz, and 1107 kHz emissions, respectively. These spatial variations do not seem to have their origin only in the distance to the antennas since we found no significant correlations between the electric field levels and the distance to each antenna. But the strong correlation ($r = 0.922$) found between the 774 kHz and 1017 kHz electric fields, and the distribution of the values shown in the spatial models that were generated, together suggest that shielding by the buildings plays a dominant part in this scenario. All the measured values of the electric fields complied with the ICNIRP guidelines for general public exposure, with even the worst case being more than 10 times below the exposure limits.

We quantified the accuracy in an urban area of three different spatial models (IDW, spline and ordinary kriging) for three different emissions and for Q_E. To calculate the accuracy of the spatial models, their electric field predictions were compared with actual measurements at 18 control points which were not used for the generation of the models. All three of the models reproduced the measured levels acceptably. However, the models that stood out for their lower RMSE values were ordinary kriging for the 774 kHz frequency and IDW for the 900 kHz and 1107 kHz emissions. In linear fits of the estimated electric field values to the measured values, the best regression coefficients, r, corresponded to the IDW model.

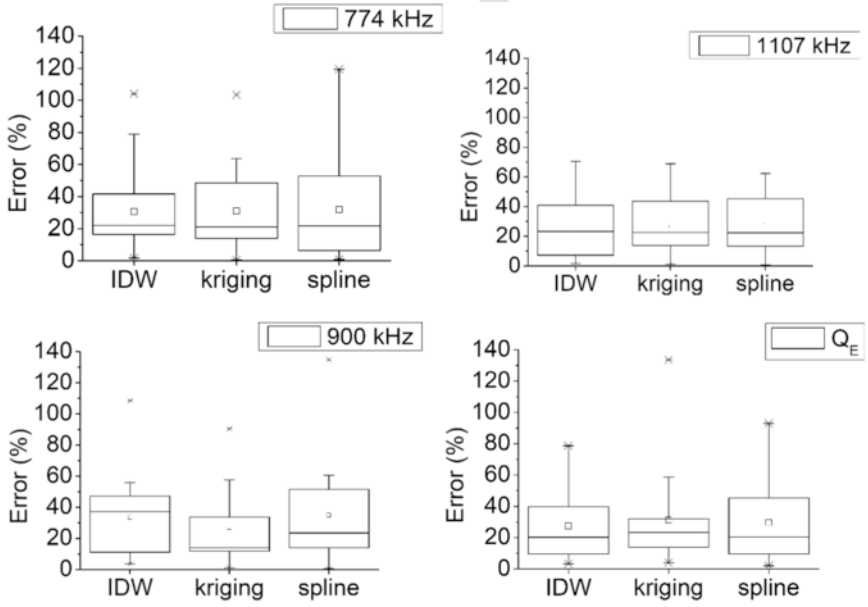

Fig. 7. Box and whisker plots of the percentage of error in the electric field evaluated and in Q_E, Eq. (10).

References

Aerts, S., Deschrijver, D., Verloock, L., Dhaene, T., Martens, L., Joseph, W., 2013. Assessment of outdoor radiofrequency electromagnetic field exposure through hotspot localization using kriging-based sequential sampling. Environ. Res. 126, 184–191. https://doi.org/10.1016/j.envres.2013.05.005.

Aminu, M., Matori, A.-N., Yusof, K.W., Malakahmad, A., Zainol, R.B., 2015. A GIS-based water quality model for sustainable tourism planning of Bertam River in Cameron Highlands, Malaysia. Environ. Earth Sci. 73, 6525–6537. https://doi.org/10.1007/s12665-014-3873-6.

Azpurua, M., dos Ramos, K., 2010. A comparison of spatial interpolation methods for estimation of average electromagnetic field magnitude. Prog. Electromagn. Res. M 14, 135–145.

Bennett, N.D., Croke, B.F.W., Guariso, G., Guillaume, J.H.A., Hamilton, S.H., Jakeman, A.J., Marsili-Libelli, S., Newham, L.T.H., Norton, J.P., Perrin, C., Pierce, S.A., Robson, B., Seppelt, R., Voinov, A.A., Fath, B.D., Andreassian, V., 2013. Characterising performance of environmental models. Environ. Model. Softw. 40, 1–20. https://doi.org/10.1016/j.envsoft.2012.09.011.

Bhatt, C.R., Redmayne, M., Abramson, M.J., Benke, G., 2016. Instruments to assess and measure personal and environmental radiofrequency-electromagnetic field exposures. Australas. Phys. Eng. Sci. Med. 39, 29–42. https://doi.org/10.1007/s13246-015-0412-z.

Bhatt, C.R., Thielens, A., Billah, B., Redmayne, M., Abramson, M.J., Sim, M.R., Vermeulen, R., Martens, L., Joseph, W., Benke, G., 2016. Assessment of personal exposure from radiofrequency-electromagnetic fields in Australia and Belgium using on-body calibrated exposimeters. Environ. Res. 151, 547–563. https://doi.org/10.1016/j.envres.2016.08.022.

Calvente, I., Fernandez, M.F., Perez-Lobato, R., Davila-Arias, C., Ocon, O., Ramos, R., Rios-Arrabal, S., Villalba-Moreno, J., Olea, N., Nunez, M.I., 2015. Outdoor characterization of radio frequency electromagnetic fields in a Spanish birth cohort. Environ. Res. 138, 136–143. https://doi.org/10.1016/j.envres.2014.12.013.

Cleveland, R.F., Ulcek, J.J.L., 1999. Questions and answers about biological effects and potential hazards of Radiofrequency electromagnetic fields. Off. Eng. Technol. Fed. Commun. Comm. 36.

Cressie, N.A.C., 1993. Statistics for spatial data. New York.

De Doncker, P., Dricot, J.-M., Meys, R., Hélier, M., Tabbara, W., 2006. Electromagnetic fields estimation using spatial statistics. Electromagnetics 26, 111–122. https://doi.org/10.1080/02726340500486450.

ECC, 2006.. Electronic Communication Committee. Measuring non-ionising electromagnetic radiation (9 kHz – 300 GHz). Revised Electronic Communication Committee Recommendation.

Egerstedt, M., Martin, C., 2010. Control Theoretic Splines. Princeton University Press.

Gajšek, P., Ravazzani, P., Wiart, J., Grellier, J., Samaras, T., Thuróczy, G., 2013. Electromagnetic field exposure assessment in Europe radiofrequency fields (10 MHz-6 GHz). J. Expo. Sci. Environ. Epidemiol. 1–8. https://doi.org/10.1038/jes.2013.40.

ICNIRP, 2010. Guidelines for limiting exposure to time-varying electric and magnetic fields (1 Hz to 100 kHz). Health Phys. 99, 818–836. https://doi.org/10.1097/HP.0b013e3181f06c86.

ICNIRP, 1998. ICNIRP guidelines for limiting exposure to time-varying electric, magnetic and electromagnetic fields. Health Phys. 74, 494–522. https://doi.org/10.1097/HP.0b013e3181f06c86.

IEEE Standard, C., 2005. IEEE Standard for Safety Levels with Respect to Human Exposure to Radio Frequency Electromagnetic Fields, 3kHz to 300 GHz. IEEE, New York, USA.

Jeong, D.I., St-Hilaire, A., Gratton, Y., Bélanger, C., Saad, C., 2017. A guideline to select an estimation model of daily global solar radiation between geostatistical interpolation and stochastic simulation approaches. Renew. Energy 103, 70–80. https://doi.org/10.1016/j.renene.2016.11.022.

Joseph, W., Frei, P., Roosli, M., Thuroczy, G., Gajsek, P., Trcek, T., Bolte, J., Vermeeren, G., Mohler, E., Juhasz, P., Finta, V., Martens, L., 2010. Comparison of personal radio frequency electromagnetic field exposure in different urban areas across Europe. Environ. Res. 110, 658–663. https://doi.org/10.1016/j.envres.2010.06.009.

Kirchner, J.W., Hooper, R.P., Kendall, C., Neal, C., Leavesley, G., 1996. Testing and validating environmental models. Sci. Total Environ. 183, 33–47. https://doi.org/10.1016/0048-9697(95)04971-1.

Li, J., Heap, A.D., 2014. Spatial interpolation methods applied in the environmental sciences: a review. Environ. Model. Softw. 53, 173–189. https://doi.org/10.1016/j.envsoft.2013.12.008.

Luo, W., Taylor, M.C., Parker, S.R., 2008. A comparison of spatial interpolation methods to estimate continuous wind speed surfaces using irregularly distributed data from England and Wales. Int. J. Climatol. 28, 947–959. https://doi.org/10.1002/joc.1583.

Maling, D.H., 1989. Measurements from maps: principles and methods of cartometry 577.

Paniagua, J.M., Rufo, M., Jimenez, A., Antolin, A., 2013. The spatial statistics formalism applied to mapping electromagnetic radiation in urban areas. Environ. Monit. Assess. 185, 311–322. https://doi.org/10.1007/s10661-012-2555-7.

Paniagua, J.M., Rufo, M., Jimenez, A., Antolin, A., Pachon, F.T., 2012. Estimation of uncertainties in electric field exposure from medium-frequency AM Broadcast transmitters. IEEE Trans. Instrum. Meas. 61, 122–128. https://doi.org/10.1109/tim.2011.2161013.

Paniagua, J.M., Rufo, M., Jimenez, A., Antolin, A., Pinar, I., 2010. Medium wave exposure characterisation using exposure quotients. Radiat. Prot. Dosim. 140, 34–40. https://doi.org/10.1093/rpd/ncq014.

Paniagua, J.M., Rufo, M., Jimenez, A., Antolin, A., Sanchez, M., 2009. Electrical stimulation vs thermal effects in a complex electromagnetic environment. Sci. Total Env. 407, 4717–4722. https://doi.org/10.1016/j.scitotenv.2009.04.034.

Recommendation, C., 1999. Council recommendation of 12 July 1999 on the limitation of exposure of the general public to electromagnetic fields (0 Hz to 300 GHz). Communities 59–70.

Royal Decree, 1993. Royal Decree 765/1993 which approved the Technical National Plan of Medium Wave Radio Broadcasting (MF), May 1993. In Spanish.

Rufo, M.M., Paniagua, J.M., Jimenez, A., Antolin, A., 2011. Exposure to high-frequency electromagnetic fields (100 kHz-2 GHz) in Extremadura (Spain). Health Phys. 101, 739–745. https://doi.org/10.1097/HP.0b013e31821fd1ec.

Seybold, J.S. Introduction to RF propagation, new Jersey. ed Introd. RF Propag. 2005 doi: ⟨http://dx.doi.org/10.1002/0471743690⟩.

Tiengrod, P., Wongseree, W., IEEE, 2013. A Comparison of spatial interpolation methods for surface temperature in Thailand. 2013 International Comput. Sci. Eng. Conference 174–178.